Lattice Decoding for Joint Detection in Direct-Sequence CDMA Systems

Loïc Brunel, *Member, IEEE*, and Joseph J. Boutros, *Member, IEEE*

***Abstract*—A new joint detection method based on sphere packing lattice decoding is presented in this paper. The algorithm is suitable for both synchronous and asynchronous multiple access direct-sequence code-division multiple-access (DS-CDMA) systems, and it may jointly detect up to 64 users with a reasonable complexity. The detection complexity is independent of the modulation size and large M-PAM or M-QAM constellations can be used. Furthermore, a theoretical gain analysis is performed in which the multiple-access system performance is derived from the lattice parameters.**

***Index Terms*—Code-division multiple access (CDMA), lattice decoding, multiuser detection, sphere decoder.**

I. Introduction

In this correspondence, a new low-complexity joint detection algorithm for direct sequence (DS) multiple-access systems is proposed. The algorithm is optimal (in the maximum-likelihood (ML) sense) for synchronous code-division multiple-access (CDMA) systems. The receiver models the despreader output as a multidimensional lattice point (sphere packing) corrupted by noise and applies a lattice-decoding algorithm to jointly detect all users. In the asynchronous case, the lattice decoder is combined with an interference canceler and its performance remains excellent despite its suboptimality.

The paper is organized as follows. In Section II, the synchronous multiple-access transmitter structure and its lattice representation are described. In Section III, the sphere-decoding algorithm, which is a low-complexity ML decoder for lattice constellations, is presented. Then, sphere decoding is applied to ML detection of synchronous direct-sequence spread-spectrum multiple access (DS-SSMA) in Section IV. In Section V, the combination of sphere decoding and interference cancellation for the joint demodulation of asynchronous DS-SSMA is investigated. In Section VI, an analytical approximation for the system gain is derived from the lattice parameters. Simulation results for synchronous and asynchronous systems on additive white Gaussian noise (AWGN) channel are presented in Section VII and compared with those of multistage successive interference cancellation (PIC) [13], [14], decision-feedback minimum mean-square error detector (DF-MMSE) [9], and Viterbi-based algorithm (Verdú joint detector [15]). Conclusions are finally drawn in Section VIII.

II. Lattice Representation of Synchronous Multiuser Systems

Let us first consider a synchronous CDMA system with K users. The symbol $b_k(i)$ of user k transmitted at time i is taken from an integer alphabet $\mathcal{A}$ of cardinality $|\mathcal{A}|$. Each user k transmits a block of N symbols with signal amplitude ω_k. The symbols are spread by a real signature $s_k(t)$ with symbol duration T, $s_k(t) = 0$ if $t \notin [0, T)$. The K transmitted data symbols are placed in a row vector $\boldsymbol{b}(i)$ defined as $\boldsymbol{b}(i) = (b_1(i), \ldots, b_K(i))$. The corresponding modulated signal is

$$S_t = \sum_{i=0}^{N-1} \sum_{k=1}^{K} \omega_k b_k(i) s_k(t - iT).$$

We assume that the channel is an ideal AWGN channel. Let $r_t = S_t + \eta_t$ be the received signal and η_t a real Gaussian noise with zero mean and variance N_0. A sufficient statistic for ML detection of $\boldsymbol{b}(i)$ is $\boldsymbol{y}(i) = (y_1(i), \ldots, y_K(i))$, where $y_k(i)$ is the matched filter output of user k defined as

$$\begin{aligned} y_k(i) &\triangleq \int_{-\infty}^{+\infty} s_k(t - iT) r(t)\, dt + n_k(i) \\ &= \sum_{\ell=1}^{K} \omega_\ell b_\ell(i) \int_0^T s_\ell(t) s_k(t)\, dt + n_k(i). \end{aligned} \tag{1}$$

The cross-correlation coefficients of the noise vector $\boldsymbol{n}(i) = (n_1(i), \ldots, n_K(i))$ are

$$E[n_\ell(i) n_k(i)] = R_{\ell k} N_0, \quad \text{with } R_{\ell k} = \int_0^T s_\ell(t) s_k(t)\, dt \ \text{ for } k, \ell = 1 \cdots K. \tag{2}$$

Let $\boldsymbol{D}_\omega$ be the diagonal matrix $\mathrm{Diag}(\omega_1, \ldots, \omega_K)$ and $\boldsymbol{R} = [R_{\ell k}]$ the $K \times K$ signature cross-correlation matrix. Then, (1) becomes

$$\boldsymbol{y}(i) = \boldsymbol{b}(i)\boldsymbol{M} + \boldsymbol{n}(i) \tag{3}$$

where the $K \times K$ matrix $\boldsymbol{M}$ is defined as $\boldsymbol{M} = \boldsymbol{D}_\omega \boldsymbol{R}$.

The vector $\boldsymbol{y}(i)$ in (3) can be viewed as a point of a K-dimensional lattice sphere packing Λ [6] with generator matrix $\boldsymbol{M}$ corrupted by a noise $\boldsymbol{n}(i)$. If the signatures are well chosen and all power amplitudes are strictly positive, the lattice Λ is a $\mathbb{Z}$-module of rank K of the K-dimensional real space $\mathbb{R}^K$. The rows of $\boldsymbol{M}$ form a basis of Λ. The multiple-access signal generates a point $\boldsymbol{b}(i)\boldsymbol{M}$ belonging to a constellation, i.e., a finite subset of Λ of size $|\mathcal{A}|^K$.

This lattice representation of multiuser systems allows us to use an efficient ML lattice decoding algorithm called the *Universal Lattice Decoder* [17], [18], also known as the *Sphere Decoder* [3]. The sphere decoder is capable of decoding any lattice defined by an arbitrary generator matrix $\boldsymbol{M}$. The version presented in the following is based on enumerating points inside a sphere according to the Pohst strategy [10], [7]. Alternative strategies are presented in a recent tutorial by Agrell *et al.* [1].

III. Sphere Decoding With White Gaussian Noise

Let us first describe the ML decoding of a K-dimensional lattice Λ used over an AWGN channel and generated by a real $K \times K$ matrix $\boldsymbol{G}$. The decoder must find the closest lattice point to the received vector, which is equivalent to minimizing the metric

$$m(\boldsymbol{y}|\boldsymbol{x}) = \sum_{i=1}^{K} |y_i - x_i|^2 = \|\boldsymbol{y} - \boldsymbol{x}\|^2 \tag{4}$$

where $\boldsymbol{y} = \boldsymbol{x} + \boldsymbol{\eta}$ is the received vector, $\boldsymbol{\eta} = (\eta_1, \ldots, \eta_K)$ is the noise vector and $\boldsymbol{x} = (x_1, \ldots, x_K)$ is a point belonging to Λ. The noise vector $\boldsymbol{\eta}$ has real Gaussian distributed independent components with zero mean and variance σ^2. The lattice points $\{\boldsymbol{x} = \boldsymbol{b}\boldsymbol{G}\}$ are obtained from the data vectors $\boldsymbol{b} = (b_1, \ldots, b_K)$ where the components b_i belong to the ring of integers $\mathbb{Z}$.

Manuscript received April 17, 1999; revised December 12, 2002. The material in this correspondence was presented in part at the IEEE Information Theory Workshop, Kruger National Park, South Africa, June 1999.

L. Brunel was with the Ecole Nationale Supérieure des Télécommunications (ENST), Paris, France. He is now with Mitsubishi Electric ITE, Rennes, France (e-mail: brunel@tcl.ite.mee.com).

J. J. Boutros is with Ecole Nationale Supérieure des Télécommunications (ENST), Paris Cedex 13, France (e-mail: boutros@enst.fr).

Communicated by T. Fuja, Associate Editor At Large.

Digital Object Identifier 10.1109/TIT.2003.809506

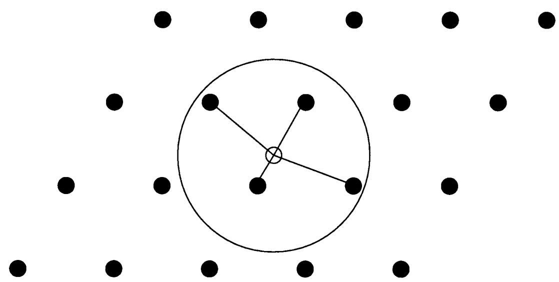

Fig. 1. Geometrical representation of the sphere-decoding algorithm.

In practice, the set of data vectors is limited to an alphabet $\mathcal{A}^K \subset \mathbb{Z}^K$ and an exhaustive ML decoder looks for the best point $\boldsymbol{x}$ in the whole finite constellation. The sphere decoder restricts its computation to the points which are found inside a sphere of a given radius $\sqrt{C}$ centered at the received point, as depicted in Fig. 1. Thus, only the lattice points within the squared distance C from the received point are considered in the metric minimization of (4). The decoder performs the following optimization:

$$\min_{\boldsymbol{x}\in\Lambda} \|\boldsymbol{y}-\boldsymbol{x}\| = \min_{\boldsymbol{w}\in\boldsymbol{y}-\Lambda} \|\boldsymbol{w}\|. \tag{5}$$

The equality (5) indicates that we must find the shortest vector $\boldsymbol{w}$ in the translated set $\boldsymbol{y}-\Lambda$. We write the received vector and the difference as $\boldsymbol{y}=\boldsymbol{\rho G}$ and $\boldsymbol{w}=\boldsymbol{\xi G}$, respectively, with $\boldsymbol{\xi}=(\xi_1,\ldots,\xi_K)\in\mathbb{R}^K$ and $\boldsymbol{\rho}=(\rho_1,\ldots,\rho_K)\in\mathbb{R}^K$.

In the new coordinate system defined by $\boldsymbol{\xi}$, the sphere of squared radius C centered at $\boldsymbol{y}$ is transformed into an ellipsoid centered at the origin, defined by

$$\|\boldsymbol{w}\|^2 = \boldsymbol{\xi G G}^T\boldsymbol{\xi}^T \le C. \tag{6}$$

Cholesky's factorization [5] of the Gram matrix $\boldsymbol{\Gamma}=\boldsymbol{GG}^T$ yields $\boldsymbol{\Gamma}=\boldsymbol{AA}^T$, where $\boldsymbol{A}$ is a lower triangular matrix with elements a_{ij}. Using (6), it was shown that point $\boldsymbol{x}$ is included in the search sphere if and only if the integer components of $\boldsymbol{b}$ satisfy the following inequalities [17], [18]:

$$\begin{aligned}
&\left\lceil -\sqrt{\frac{C}{q_{KK}}}+\rho_K\right\rceil \le b_K \le \left\lfloor \sqrt{\frac{C}{q_{KK}}}+\rho_K\right\rfloor\\
&\left\lceil -\sqrt{\frac{C-q_{KK}\xi_K^2}{q_{K-1,K-1}}}+\rho_{K-1}+q_{K,K-1}\xi_K\right\rceil\\
&\quad\le b_{K-1}\le \left\lfloor \sqrt{\frac{C-q_{KK}\xi_K^2}{q_{K-1,K-1}}}+\rho_{K-1}+q_{K,K-1}\xi_K\right\rfloor\\
&\left\lceil -\sqrt{\frac{1}{q_{ii}}\left(C-\sum_{\ell=i+1}^{K}q_{\ell\ell}\left(\xi_\ell+\sum_{j=\ell+1}^{K}q_{j\ell}\xi_j\right)^2\right)}\right.\\
&\quad\left.+\rho_i+\sum_{j=i+1}^{K}q_{ji}\xi_j\right\rceil\le b_i\\
&b_i\le\left\lfloor \sqrt{\frac{1}{q_{ii}}\left(C-\sum_{\ell=i+1}^{K}q_{\ell\ell}\left(\xi_\ell+\sum_{j=\ell+1}^{K}q_{j\ell}\xi_j\right)^2\right)}\right.\\
&\quad\left.+\rho_i+\sum_{j=i+1}^{K}q_{ji}\xi_j\right\rfloor
\end{aligned}\tag{7}$$

where $q_{ii}=a_{ii}^2$ for $i=1,\ldots,K$ and $q_{ij}=a_{ij}/a_{ii}$ for $j=1,\ldots,K$, $i=j+1,\ldots,K$. The function $\lceil x\rceil$ is the *ceil* function and $\lfloor x\rfloor$ is the *floor* function. The lower and upper bounds in (7) tell us that the sphere decoder has K internal counters b_i, i.e., one counter per dimension. We, thus, enumerate all values of vector $\boldsymbol{b}$ for which the corresponding lattice point $\boldsymbol{x}=\boldsymbol{bG}$ is within the squared distance C from the received point. Lattice points outside the given sphere are never tested. Consequently, the decoding complexity does not depend on the size $|\mathcal{A}|^K$ of the lattice constellation. Finally, we select the best point $\boldsymbol{x}$ as the one associated to the minimal Euclidean norm $\|\boldsymbol{w}\|$. During the enumeration of all points located in the search sphere, the radius $\sqrt{C}$ may be updated by the norm $\|\boldsymbol{w}\|$ found at the current enumerated point. Points located in the initial sphere beyond the updated radius are not selected by the decoder. The update of $\sqrt{C}$ by every newly computed $\|\boldsymbol{w}\|$ guarantees that all points in the new search sphere have a norm smaller or equal to $\|\boldsymbol{w}\|$. Thus, the points in this sphere are good candidates for ML detection. This radius update dramatically accelerates the closest point search.

For more details on the sphere decoding implementation, the reader is referred to [18].

The search radius $\sqrt{C}$ must be properly chosen. Indeed, the number of lattice points lying inside the decoding sphere increases with C. Therefore, a large value of C slows down the algorithm, whereas the search sphere may be empty if C is chosen too small. In order to ensure that at least one lattice point is found by the sphere decoder, the search radius has to be greater than the lattice covering radius, e.g., select a radius value equal to the Rogers upper bound [6]

$$\sqrt{C}^K = (K\log K + K\log\log K + 5K)\times\frac{|\det(\boldsymbol{G})|}{V_K}$$

where V_K is the volume of a sphere of radius 1 in the real space $\mathbb{R}^K$. As we consider a finite constellation of the lattice, it may occur that no lattice point in the sphere belongs to the constellation. This decoding failure is overcome by slightly increasing the search radius and performing the sphere decoding again.

IV. Decoding of a Synchronous Multiple-Access System

The additive-noise samples included in the system model (3) are correlated. This correlation is produced by the nonzero cross correlation between the different users signatures, see (2). The ML lattice decoder must minimize the following metric:

$$m'(\boldsymbol{y}(i)|\boldsymbol{x}(i)) = (\boldsymbol{y}(i)-\boldsymbol{x}(i))\boldsymbol{R}^{-1}(\boldsymbol{y}(i)-\boldsymbol{x}(i))^T. \tag{8}$$

The sphere-decoder equations can be easily adapted to the optimization of metric (8). This is equivalent to ML decoding of a lattice Λ' with a generator matrix $\boldsymbol{M}$ in the presence of colored noise $\boldsymbol{n}(i)$. Nevertheless, we prefer to whiten the noise at the output of the matched filter bank in order to use the decoding procedure given in the preceding section. Note that all studies of lattice sphere packing performance have been done in the AWGN case. The noise whitening will also help us to simplify the analytical study of lattice parameters' impact on the CDMA error rate presented in Section VI.

The noise whitening operation performed before the lattice decoder is similar to what is widely known in equalization theory [12]. Cholesky factorization of the cross-correlation matrix $\boldsymbol{R}$ yields $\boldsymbol{R}=\boldsymbol{WW}^T$, where $\boldsymbol{W}$ is a lower triangular matrix. The whitened observation is defined as $\tilde{\boldsymbol{y}}(i)=\boldsymbol{y}(i)\boldsymbol{W}^{T^{-1}}$ and the new lattice point is given by $\tilde{\boldsymbol{x}}(i)=\boldsymbol{x}(i)\boldsymbol{W}^{T^{-1}}$. Finally, the whole CDMA system model is illustrated in Fig. 2.

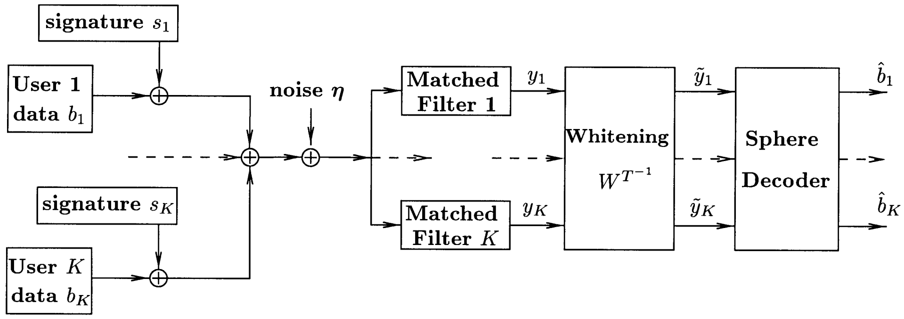

Fig. 2. CDMA system model with joint lattice detection.

Now, we write the relation between the lattice point $\tilde{\boldsymbol{x}}(i)$ and the data vector $\boldsymbol{b}(i)$

$$\tilde{\boldsymbol{x}}(i) = \boldsymbol{x}(i)\boldsymbol{W}^{T^{-1}} = \boldsymbol{b}(i)\boldsymbol{M}\boldsymbol{W}^{T^{-1}} = \boldsymbol{b}(i)\boldsymbol{D_\omega W}. \tag{9}$$

Equation (9) shows that the whitening operation results in a new lattice with generator matrix $\boldsymbol{G} = \boldsymbol{D}_\omega \boldsymbol{W}$. Therefore, the new received point $\tilde{\boldsymbol{y}}(i)$ is processed with a sphere decoder associated to this new lattice. Since $\boldsymbol{D}_\omega \boldsymbol{W}$ is already a lower triangular matrix, Cholesky factorization preceding the sphere search given by inequalities (7) can be omitted ($\boldsymbol{A} = \boldsymbol{G}$), or equivalently, the triangular factorization has been transferred from the decoder to the noise whitener.

V. Sphere Decoding With Interference Cancellation for Asynchronous Multiuser Systems

Let us now consider an asynchronous multiuser system. User k has a delay τ_k. We assume that $0 \leq \tau_1 \leq \tau_2 \leq \cdots \leq \tau_K < T$. As shown in Fig. 3, each symbol of a given user interferes with one or two symbols from other users. The latter symbols interfere also with other symbols and it is impossible to define a finite-dimensional lattice to describe the system as we did in Section II. To solve this problem, we combine the lattice decoder with a subtractive interference canceler. The detection of symbol $b_k(i)$ takes into account its entire despreading, the partial despreading of future symbols of other users, and the partial correlations with past symbols of other users.

The joint processing of symbols $b_j(i)$ at time i starts after finishing the detection of all symbols $b_j(i-1)$, $j = 1 \cdots K$. The detection at time i is performed in an increasing order of k, i.e., the demodulation of $b_k(i)$ uses the symbols $b_1(i), b_2(i), \ldots, b_{k-1}(i)$ already detected and the previous symbols $b_{k+1}(i-1), b_{k+2}(i-1), \ldots, b_K(i-1)$. The detection procedure for a given user k at time i depends on three vectors: the past symbols $\boldsymbol{b_p}$, the future symbols $\boldsymbol{b_f}$, and the observation vector $\boldsymbol{y_f} = (y_{f1}, \ldots, y_{fK})$. The symbol vectors are

$$\begin{aligned}\boldsymbol{b_p} &= (b_{p1}, \ldots, b_{pK})\\ &= (b_1(i), \ldots, b_{k-1}(i), b_k(i-1), b_{k+1}(i-1), \ldots, b_K(i-1))\\ \boldsymbol{b_f} &= (b_{f1}, \ldots, b_{fK})\\ &= (b_1(i+1), \ldots, b_{k-1}(i+1), b_k(i), b_{k+1}(i), \ldots, b_K(i)).\end{aligned}$$

When decoding symbol $b_k(i)$, the observation $y_{f\ell}$ associated to $b_{f\ell}$ is the result of a partial despreading of duration $t_{k\ell}$, beginning with symbol $b_{f\ell}$ and ending with symbol $b_k(i)$. Thus,

$$\begin{aligned}t_{k\ell} &= \tau_k - \tau_\ell, && \text{for } \ell < k\\ t_{k\ell} &= T + \tau_k - \tau_\ell, && \text{for } \ell \geq k.\end{aligned}$$

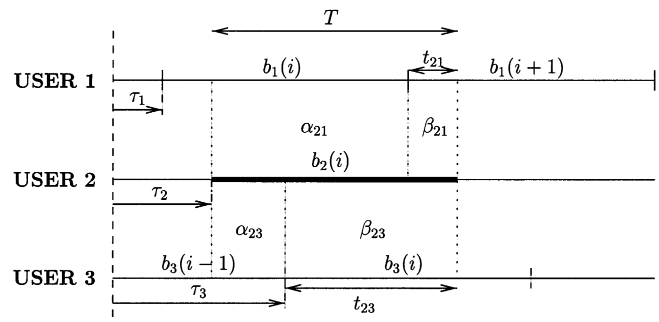

Fig. 3. Asynchronous multiple-access system with three users: interference on user 2.

Let $\beta_{j\ell}$ denote the cross correlation between symbols b_{fj} and $b_{f\ell}$. Let $\alpha_{j\ell}$ denote the cross correlation between symbol $b_j(i)$ and the previously detected symbol of user ℓ. We can express the observation vector $\boldsymbol{y_f} = (y_{f1}, \ldots, y_{fK})$ associated to the detection of $b_k(i)$ as

$$\begin{aligned}y_{fj} &= \omega_j\beta_{jj}b_{fj} + \sum_{j<\ell<k}\omega_\ell\alpha_{j\ell}b_{p\ell} + \sum_{\ell\neq j}\omega_\ell\beta_{j\ell}b_{f\ell} + n_j, \\ &\qquad\qquad \text{for } j < k\\ y_{fj} &= \omega_j\beta_{jj}b_{fj} + \sum_{\ell\neq j}\omega_\ell\alpha_{j\ell}b_{p\ell} + \sum_{\ell\neq j}\omega_\ell\beta_{j\ell}b_{f\ell} + n_j, \\ &\qquad\qquad \text{for } j = k\\ y_{fj} &= \omega_j\beta_{jj}b_{fj} + \sum_{\ell<k}\omega_\ell\alpha_{j\ell}b_{p\ell} + \sum_{\ell>j}\omega_\ell\alpha_{j\ell}b_{p\ell}\\ &\quad + \sum_{\ell\neq j}\omega_\ell\beta_{j\ell}b_{f\ell} + n_j, \qquad \text{for } j > k.\end{aligned} \tag{10}$$

Equations (10) can be simply written in matrix form

$$\boldsymbol{y_f} = \boldsymbol{b_p D_\omega R_p} + \boldsymbol{b_f D_\omega R_f} + \boldsymbol{n} \tag{11}$$

where $\boldsymbol{R_f} = [\beta_{ij}]$, $\boldsymbol{n}$ is an additive Gaussian noise with covariance matrix $N_0\boldsymbol{R_f}$, and $\boldsymbol{R_p}$ is given in the equation at the top of the following page.

There exist K different pairs of matrices $\boldsymbol{R_p}$ and $\boldsymbol{R_f}$, each one for the detection of one user. Symbols included in $\boldsymbol{b_p}$ are already detected, so we can subtract the past interference $\boldsymbol{b_p D_\omega R_p}$ from the observation $\boldsymbol{y_f}$ to obtain a new observation $\boldsymbol{z_f}$ delivered to the lattice decoder

$$\boldsymbol{z_f} = \boldsymbol{y_f} - \boldsymbol{b_p D_\omega R_p} = \boldsymbol{b_f D_\omega R_f} + \boldsymbol{n}.$$

The vector $\boldsymbol{z_f}$ is a lattice point corrupted with colored noise. Hence, we can apply results of Section IV to detect $b_k(i)$ using a sphere decoder in the K-dimensional real space. Note that K lattice-decoding steps are needed to demodulate the K users at a given time i, whereas one decoding step suffices to jointly decode all users in the synchronous system.

$$
\boldsymbol{R_p} = \begin{bmatrix}
0 & 0 & 0 & \cdots & 0 & 0 & \alpha_{1,\,k} & \alpha_{1,\,k+1} & & \cdots & \alpha_{1,\,K} \\
\alpha_{2,\,1} & 0 & 0 & \cdots & 0 & 0 & \alpha_{2,\,k} & \alpha_{2,\,k+1} & & \cdots & \alpha_{2,\,K} \\
\alpha_{3,\,1} & \alpha_{3,\,2} & 0 & \cdots & 0 & 0 & & & & & \\
\vdots & & \ddots & \ddots & \vdots & \vdots & \vdots & \vdots & & & \vdots \\
\alpha_{k-2,\,1} & \alpha_{k-2,\,2} & \cdots & \alpha_{k-2,\,k-3} & 0 & 0 & \alpha_{k-2,\,k} & \alpha_{k-2,\,k+1} & & \cdots & \alpha_{k-2,\,K} \\
\alpha_{k-1,\,1} & \alpha_{k-1,\,2} & \cdots & \alpha_{k-1,\,k-3} & \alpha_{k-1,\,k-2} & 0 & \alpha_{k-1,\,k} & \alpha_{k-1,\,k+1} & \cdots & & \alpha_{k-1,\,K} \\
0 & 0 & \cdots & 0 & 0 & 0 & 0 & 0 & 0 & \cdots & 0 \\
0 & & \cdots & & 0 & 0 & \alpha_{k+1,\,k} & 0 & 0 & \cdots & 0 \\
0 & & & & 0 & 0 & \alpha_{k+2,\,k} & \alpha_{k+2,\,k+1} & 0 & & 0 \\
\vdots & & & & \vdots & \vdots & \vdots & & \ddots & \ddots & \vdots \\
0 & 0 & \cdots & 0 & 0 & 0 & \alpha_{K-1,\,k} & \alpha_{K-1,\,k+1} & \cdots & \alpha_{K,\,K-1} & 0
\end{bmatrix}.
$$

VI. Analytical Performance Derived From the Lattice Parameters

We now compute an analytical bound for the system gain by studying the structure of the embedded lattice constellation. For simplicity reasons, it is assumed that all users are synchronous and that the multiple-access medium is an ideal AWGN channel. The point error probability P_e of a cubic constellation S is approximated by [4]

$$P_e \approx \frac{\tau(\Lambda)}{2}\,\mathrm{erfc}\left(\sqrt{\frac{3\zeta}{2^{\zeta+1}}\,\frac{E_b}{N_0}\,\gamma(\Lambda)}\right)$$

where $\tau(\Lambda)$ is the first shell population number (*kissing number*), erfc is the complementary error function, ζ is the number of bits per two dimensions, E_b is the bandpass average energy per bit. The *fundamental gain* $\gamma(\Lambda)$ is given by [8]

$$\gamma(\Lambda) = \frac{d^2_{\mathrm{E\,min}}}{\mathrm{vol}(\Lambda)^{2/K}} \tag{12}$$

for a K-dimensional lattice with minimal Euclidean distance $d_{\mathrm{E\,min}}$ and a fundamental volume $\mathrm{vol}(\Lambda)$. The fundamental gain, also known as Hermite constant [6], is equivalent to the normalized Euclidean distance of a trellis-coded modulation [2], and gives its asymptotic signal-to-noise ratio (SNR) gain. If $\boldsymbol{G}$ is the generator matrix of Λ, $\mathrm{vol}(\Lambda) = |\det(\boldsymbol{G})|$. The energy ratio $\gamma(\Lambda)$ stands for the gain of Λ when the integer lattice $\mathbb{Z}^K$ is taken as a reference. Recall that $\gamma(\mathbb{Z}^K) = 1$ and that $\gamma(\Lambda)$ depends only on the lattice structure. When the constellation S is not of cubic shape, the total gain $\gamma(S)$ is equal to the product of the fundamental gain and the *shaping gain* $\gamma_s(S)$, where the latter depends on the constellation second moment [8]

$$\gamma(S) = \gamma(\Lambda) \times \gamma_s(S).$$

Let $\overline{\|\boldsymbol{b}\|^2_{\mathrm{cube}}}$ be the second moment of the integer constellation S_{cube} obtained from the concatenation of the K users' symbols. Let $\overline{\|\tilde{\boldsymbol{x}}\|^2_S}$ be the second moment of the constellation S. We assume that S and S_{cube} have the same volume. Thus, (9) becomes

$$\tilde{\boldsymbol{x}} = \boldsymbol{b}\boldsymbol{G}/\sqrt[K]{|\det(\boldsymbol{G})|}$$

and a simple calculation gives the formula of the shaping gain

$$\gamma_s(S) = \frac{\overline{\|\boldsymbol{b}\|^2_{\mathrm{cube}}}}{\overline{\|\tilde{\boldsymbol{x}}\|^2_S}} = \frac{K \cdot \sqrt[K/2]{\det(\boldsymbol{G})}}{\mathrm{Trace}(\boldsymbol{\Gamma})}. \tag{13}$$

Now, let us study the simple case of a synchronous $K = 2$ users system. We assume that user 1 has unit amplitude and user 2 has amplitude $\omega \geq 1$. The cross-correlation coefficient is denoted $\beta \in [0,\,1]$. Then, the cross-correlation matrix $\boldsymbol{R}$ and the generator matrix of the associated lattice are

$$\boldsymbol{R} = \begin{bmatrix} 1 & \beta \\ \beta & 1 \end{bmatrix} \quad \text{and} \quad \boldsymbol{G} = \boldsymbol{D_\omega W} = \begin{bmatrix} 1 & 0 \\ \omega\beta & \omega\sqrt{1-\beta^2} \end{bmatrix}.$$

The CDMA system performance is compared to that of a reference system defined by a constellation S_o. This reference constellation is cubic shaped and corresponds to the ideal case of two orthogonal signatures ($\beta = 0$, $d^2_{\mathrm{E\,min}} = 1$); we have

$$\begin{aligned} \gamma(\Lambda_o) &= \omega^{-1} \\ \gamma_s(S_o) &= \frac{2\omega}{1+\omega^2} \\ \gamma(S_o) &= \frac{2}{1+\omega^2}. \end{aligned} \tag{14}$$

Finally, the total gain $\gamma'(S)$ of the CDMA system is defined as the ratio of $\gamma(S)$ to $\gamma(S_o)$

$$\gamma'(S) = \frac{d^2_{\mathrm{E\,min}}(1+\omega^2)}{\mathrm{Trace}(\boldsymbol{\Gamma})}. \tag{15}$$

The lattice minimum squared distance $d^2_{\mathrm{E\,min}}$ can be determined by[1]

$$d^2 = \min(1,\, \kappa^2 + \omega^2 - 2\kappa\omega\beta)$$

where κ is the nearest integer to $\omega\beta$. Thus, we can write

$$\mathrm{Trace}(\boldsymbol{\Gamma}) = \mathrm{Trace}(\boldsymbol{G}\boldsymbol{G}^T) = 1 + \omega^2. \tag{16}$$

From (15) and (16), we get a simple expression for the total gain of the multiple-access system

$$\gamma'(S) = d^2. \tag{17}$$

Consequently, as long as $d^2 = 1$, there is no global performance loss in our system. In other words, the joint detection shows a zero loss in performance for small and medium values of the correlation coefficient. The theoretical gain in (17), expressed in decibels and illustrated versus β, will be compared to the effective gain measured by computer simulation in the next section. This theoretical gain is equivalent to the asymptotic efficiency of the DS-CDMA system [16].

VII. Simulation Results

In a first scenario, the sphere-decoding algorithm has been applied to jointly detect four and seven users in a direct-sequence SSMA system. The signatures are Gold sequences with period 7 (spreading factor $= 7$). The first user has a fixed transmit power. All other users have equal transmit power and we vary their SNR to observe the near–far

[1]We would like to emphasize that in some exceptional cases, e.g., β close to 1.0, the distance d may not equal the true minimum distance

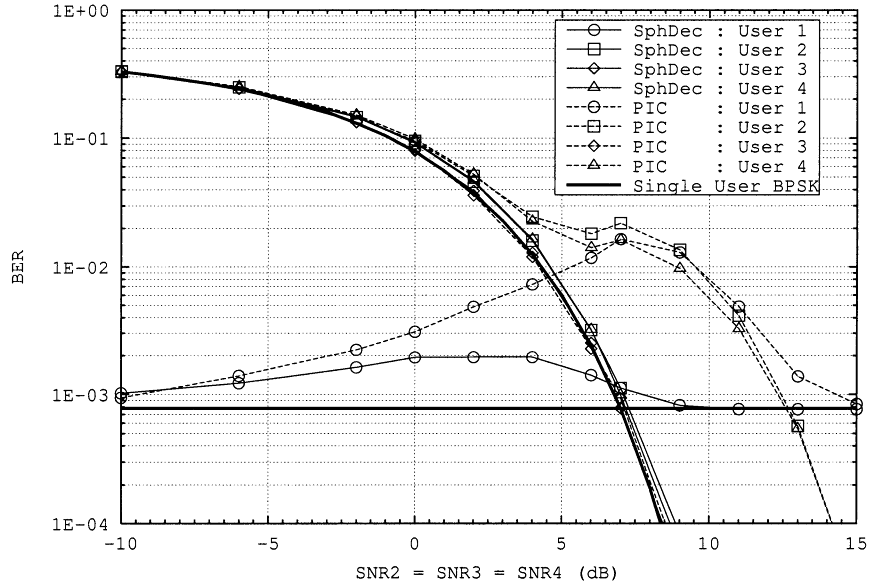

Fig. 4. Synchronous system: four users, BPSK modulation, SNR1 $=7$ dB, three iterations for PIC hard detector.

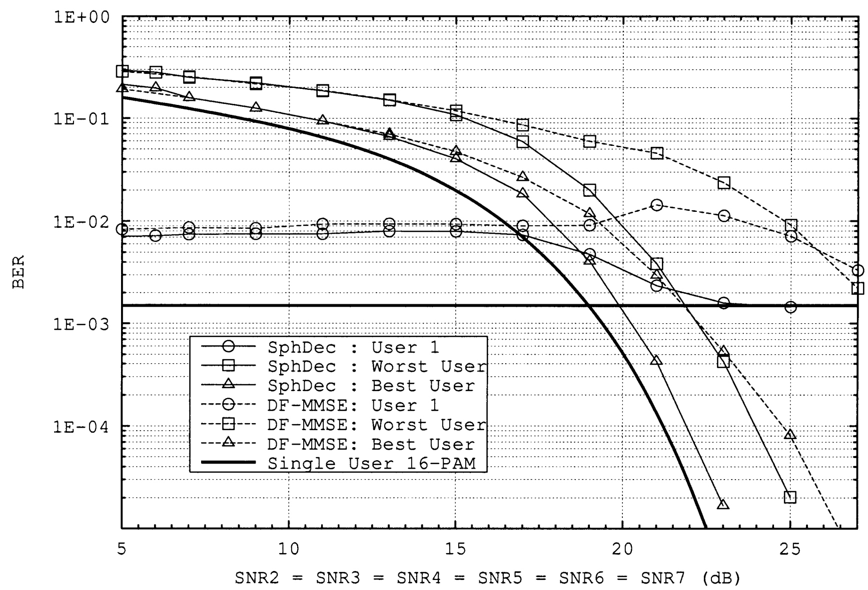

Fig. 5. Synchronous system: seven users, 16-PAM modulation, SNR1 $=19$ dB.

effect on the first user. The results are compared with those of a PIC detector with hard cancellation and a decision feedback MMSE joint equalizer. At the first iteration of the PIC detector, the contributions of interfering users are successively subtracted from the received signal by decreasing order of transmit power, which is not necessarily the optimum order. In the following iterations, parallel interference cancellation is performed. The total number of iterations is three.

Consider a model of synchronous transmission with binary phase-shift keying (BPSK) modulation on a Gaussian channel. Fig. 4 depicts the ML performance of the sphere decoder. It is very near–far resistant compared to the PIC detector. The performances of different users are similar contrary to those of the PIC which depend on the cross-correlation values. For user 4, we observe a 5.5-dB gain for the sphere decoder with respect to the PIC detector.

In Fig. 5, with a 16-PAM modulation and seven users, the sphere decoder outperforms the DF-MMSE detector. An exhaustive ML detector would have to compute $16^4 = 65\,536$ metrics to detect each point!

Tables I and II compare the complexity of the sphere decoder with that of the exhaustive search when both perform an ML joint CDMA detection. All users transmit 16-PAM signals with the same transmit power equal to 19 dB. The average complexity of the sphere decoder has been measured by counting all the operations executed in our simulation program. The lower the SNR, the larger the variance of the complexity. The search radius has been determined from Rogers bound. A further reduction of the number of operations can be achieved with the Lenstra–Lenstra–Lovasz (LLL) algorithm [5], [11], especially in a near-far effect situation.

To illustrate the relative low complexity of sphere decoding, let us consider a synchronous system with 63 users using 16-PAM modulation and spread by a factor 63. Two sets of spreading sequences are used. The first set contains 63 Gold sequences of length 63. The repartition of the nontrivial cross-correlation absolute values is: $17/63$ (12 occurrences), $15/63$ (17 occurrences), $1/63$ (3876 occurrences). The second set contains 63 highly correlated purely theoretical sequences

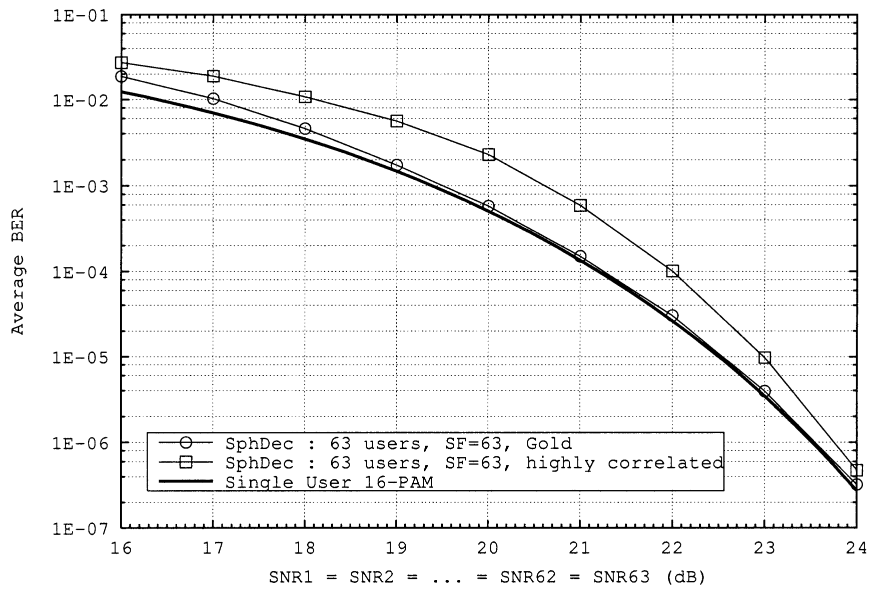

Fig. 6. Synchronous system: 63 users, 16-PAM modulation.

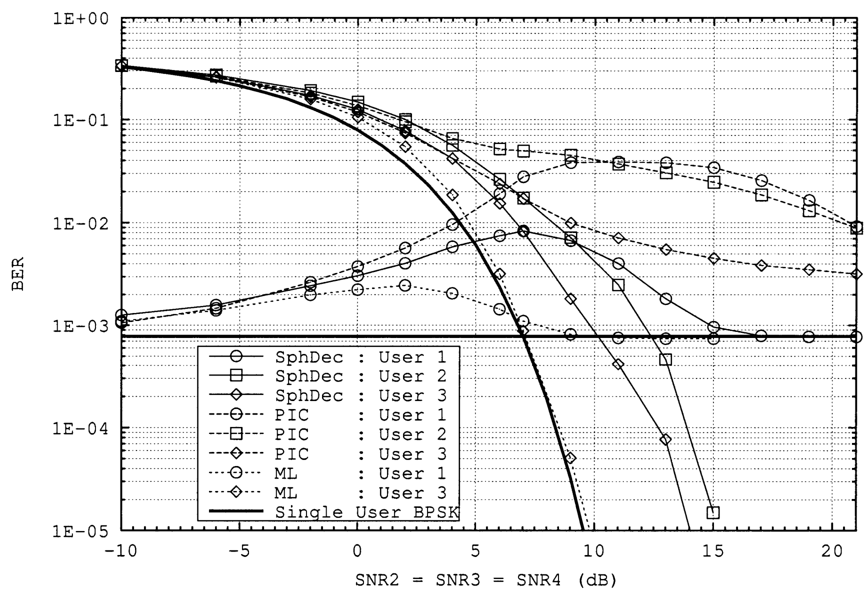

Fig. 7. Asynchronous system: four users, BPSK modulation, SNR1 $= 7$ dB, three iterations for PIC hard detector.

TABLE I
COMPLEXITY OF THE JOINT ML DETECTOR BASED ON THE SPHERE DECODER (WITHOUT LLL) FOR 16-PAM MODULATION. THE SEARCH RADIUS IS DERIVED FROM ROGERS BOUND

K	Additions per user	Multiplications per user	Divisions per user	Square Roots per user	Total per user	Total for all K users
4	111	68	14	14	208	832
7	480	332	49	49	910	6371

of length 63. In the latter case, all nontrivial cross-correlations absolute values are equal to $21/63$. All users have the same transmit power. In Fig. 6, performance results with both sequence sets are depicted versus the SNR of all users. Although the system is highly loaded, the single-user performance is reached with Gold sequences, whereas a low degradation of 0.5 dB is observed at an average bit-error rate (BER) equal to 10^{-5} when using highly correlated sequences. This shows that, even with highly correlated sequences, the ML performance is near the single-user performance, i.e., the multiuser efficiency is close to 1.

Let us now consider an asynchronous multiple-access system. The time delays are 0, 2, 4, and 6 chips for four users. The results are represented in Fig. 7. It is clear that the pure ML detector based on Viterbi

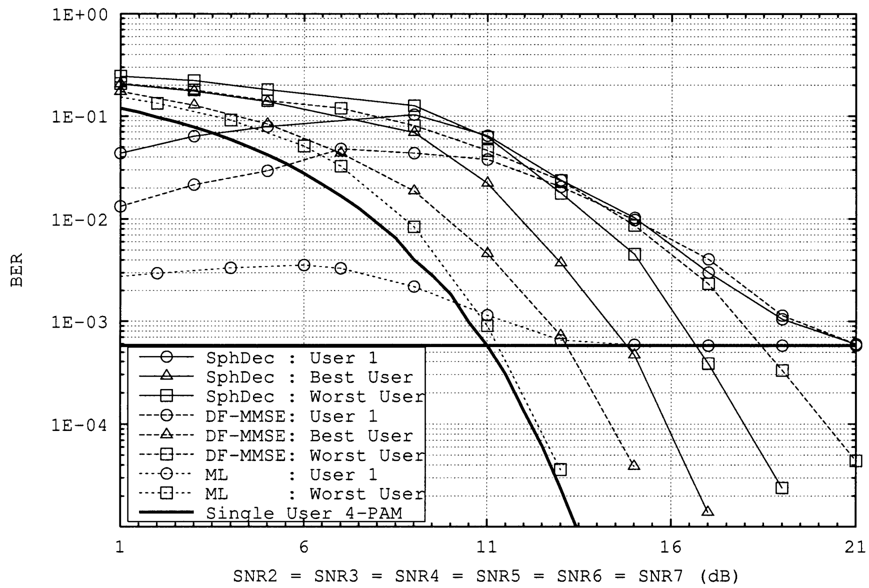

Fig. 8. Asynchronous system: seven users, 4-PAM modulation, SNR1 $= 11$ dB.

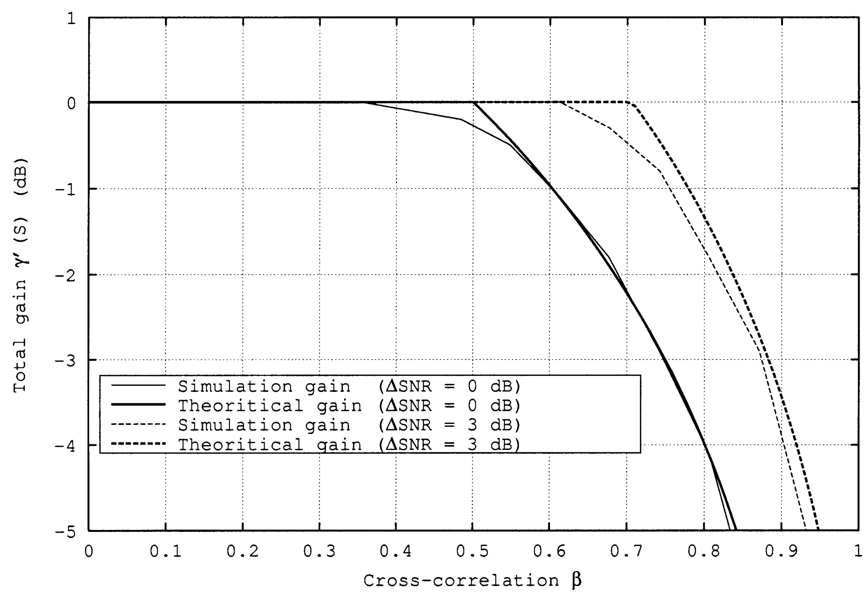

Fig. 9. Synchronous system gain: two users, 16-PAM modulation.

algorithm has the lowest error rate. However, the combination of sphere decoding and interference cancellation still outperforms the PIC detector. Fig. 8 depicts the BER with a 4-PAM asynchronous system for seven users and a spreading factor 7. The system has a full load. The sphere decoder has the best average error rate because its worst user is well protected. The DF-MMSE detector exhibits a relatively large difference between the performance of the best and the worst users.

Finally, we represented in Fig. 9 the theoretical global gain given by (17) in Section VI for two users with an SNR difference ΔSNR $= 0$ and 3 dB. This gain is compared with the one derived from computer simulations. As predicted by information theory, the bigger ΔSNR is, the higher the gain is! In fact, the strongest user has a negligible effect on the global BER. Thus, the global gain is roughly related to the weakest user. The latter is less sensitive to cross-correlation variations since its error rate is higher.

TABLE II
COMPLEXITY OF THE JOINT ML DETECTOR BASED ON EXHAUSTIVE SEARCH FOR 16-PAM MODULATION

K	Additions per user	Multiplications per user	Total per user	Total for all K users
4	10^5	10^5	2.10^5	8.10^5
7	6.10^8	6.10^8	12.10^8	8.10^9

VIII. CONCLUSION

In this correspondence, we proposed a new joint detection technique based on lattice (sphere packing) decoding using the sphere-decoding algorithm. The algorithm is optimal in synchronous systems and exhibits excellent performance when users are asynchronous. The algorithm may jointly detect up to 64 users which is a practical limit for the complexity of the sphere decoding [18]. Indeed, in the worst case, the kernel of the sphere decoder has a complexity proportional to K^6 [7]. Furthermore, the detection complexity does not depend on the modulation size and large M-PAM or M-QAM constellations can be used. We also derived a theoretical gain analysis where the performance is derived from the lattice parameters. The sphere decoder is clearly more complex than linear joint detectors, but its complexity gain is significant versus the ML exhaustive or Viterbi algorithm, especially for large modulation alphabets. The use of such modulations could be suggested to increase the spectral efficiency of DS-CDMA mobile radio systems. For example, in the European UMTS standard, the combination of several services belonging to the same user makes the final modulated signal behave like a large alphabet signal.

Finally, the authors would like to indicate that the sphere decoder is applicable to any communication system satisfying a constraint similar to (3). This includes multiantenna and multicarrier systems.

Acknowledgment

The authors wish to thank the reviewers for their useful comments which helped to greatly improve the presentation of the correspondence.

References

[1] E. Agrell, T. Eriksson, A. Vardy, and K. Zeger, “Closest point search in lattices,” *IEEE Trans. Inform. Theory*, vol. 48, pp. 2201–2214, Aug. 2002.
[2] E. Biglieri, D. Divsalar, P. J. McLane, and M. K. Simon, *Introduction to Trellis Coded Modulation with Applications*. New York: Macmillan, 1991.
[3] J. Boutros, “Lattice codes for Rayleigh fading channels,” Thèse de Doctorat, ENST, Paris, France, June 1996.
[4] J. Boutros, E. Viterbo, C. Rastello, and J. C. Belfiore, “Good lattice constellations for both Rayleigh fading and Gaussian channels,” *IEEE Trans. Inform. Theory*, vol. 42, pp. 502–518, Mar. 1996.
[5] H. Cohen, *Computational Algebraic Number Theory*. Berlin, Germany: Springer-Verlag, 1993.
[6] J. H. Conway and N. J. Sloane, *Sphere Packings, Lattices and Groups*, 3rd ed. New York: Springer-Verlag, 1998.
[7] U. Fincke and M. Pohst, “Improved methods for calculating vectors of short length in a lattice, including a complexity analysis,” *Math. Comput.*, vol. 44, pp. 463–471, Apr. 1985.
[8] G. D. Forney, Jr., “Coset codes I: Introduction and geometrical classification,” *IEEE Trans. Inform. Theory*, vol. 34, pp. 1123–1151, Sept. 1988.
[9] A. Klein, G. K. Kaleh, and P. W. Baier, “Zero forcing and minimum mean-square-error equalization for multiuser detection in code-division multiple-access channels,” *IEEE Trans. Veh. Technol.*, vol. 45, pp. 276–287, May 1996.
[10] M. Pohst, “On the computation of lattice vectors of minimal length, successive minima, reduced bases with applications,” in *ACM SIGSAM Bull*, vol. 15, Feb. 1981, pp. 37–44.
[11] M. Pohst and H. Zassenhaus, *Algorithmic Algebraic Number Theory*. Cambridge, U.K.: Cambridge Univ. Press, 1989.
[12] J. G. Proakis, *Digital Communications*, 3rd ed. New York: McGraw-Hill, 1995.
[13] M. K. Varanasi and B. Aazhang, “Multistage detection in asynchronous code division multiple access communications,” *IEEE Trans. Commun.*, vol. 38, pp. 509–519, Apr. 1990.
[14] ——, “Near-optimum detection in synchronous code division multiple access systems,” *IEEE Trans. Commun.*, vol. 39, pp. 725–735, May 1991.
[15] S. Verdú, “Minimum probability of error for asynchronous Gaussian multiple-access channels,” *IEEE Trans. Inform. Theory*, vol. IT-32, pp. 85–96, Jan. 1986.
[16] ——, “Optimum multiuser asymptotic efficiency,” *IEEE Trans. Commun.*, vol. COM–34, pp. 890–897, Sept. 1986.
[17] E. Viterbo and E. Biglieri, “A universal lattice decoder,” in *Proc. 14ème Colloque GRETSI*, Juan-les-Pins, France, Sept. 1993, pp. 611–614.
[18] E. Viterbo and J. Boutros, “A universal lattice code decoder for fading channels,” *IEEE Trans. Inform. Theory*, vol. 45, pp. 1639–1642, July 1999.

Upper Bounds on Empirically Optimal Quantizers

Dong Sik Kim, *Member, IEEE*, and Mark R. Bell, *Senior Member, IEEE*

***Abstract*—In designing a vector quantizer using a training sequence (TS), the training algorithm tries to find an *empirically optimal quantizer* that minimizes the selected distortion criteria using the sequence. In order to evaluate the performance of the trained quantizer, we can use the empirically minimized distortion that we obtain when designing the quantizer. In this correspondence, several upper bounds on the empirically minimized distortions are proposed with numerical results. The bound holds pointwise, i.e., for each distribution with finite second moment in a class. From the pointwise bounds, it is possible to derive the worst case bound, which is better than the current bounds for practical *training ratio* β, the ratio of the TS size to the codebook size. It is shown that the empirically minimized distortion underestimates the true minimum distortion by more than a factor of $(1 - 1/m)$, where m is the sequence size. Furthermore, through an asymptotic analysis in the codebook size, a multiplication factor $[1 - (1 - e^{-\beta})/\beta] \approx (1 - 1/\beta)$ for an asymptotic bound is shown. Several asymptotic bounds in terms of the vector dimension and the type of source are also introduced.**

***Index Terms*—Clustering algorithm, empirically optimal quantizer, training sequence (TS), vector quantizer.**

I. Introduction

The codewords of the vector quantizer (VQ) codebook are elements of k-dimensional Euclidean space $\mathbb{R}^k$, and the VQ design problem can be described as finding a set of codewords in $\mathbb{R}^k$ such that length k source sequences can be efficiently represented (i.e., a sufficiently small number of codewords) with an acceptably small average distortion (a statistically appropriate distribution of the codewords throughout $\mathbb{R}^k$). Let F be a distribution function, k be a fixed integer, and $\|\cdot\|$ denote the L_2 norm on $\mathbb{R}^k$. The optimal quantizer design problem for F is to find a codebook that minimizes the average distortion defined by

$$D(C) := \int \min_{\boldsymbol{y}\in C} \|\boldsymbol{x}-\boldsymbol{y}\|^2 \, dF(\boldsymbol{x}) \tag{1}$$

over all possible choices of the set C in $\mathcal{C}_n$, where $\mathcal{C}_n$ is the class of sets that contains n points. Let the sets in $\mathcal{C}_n$ be called the *codebooks*, where each codebook has n codewords. Let C^* be an optimal codebook

Manuscript received October 25, 2001; revised September 26, 2002. This work was supported under Grant R01-2001-000-00344-0(2002) from the Basic Research Program of the Korea Science and Engineering Foundation.

D. S. Kim is with the School of Electronics and Information Engineering, Hankuk University of Foreign Studies, Yongin, Kyonggi-do, 449-791, Korea (e-mail: dskim@hufs.ac.kr).

M. R. Bell is with the School of Electrical and Computer Engineering, Purdue University, West Lafayette, IN 47907-1285 USA (e-mail: mrb@ecn.purdue.edu).

Communicated by R. Zamir, Associate Editor for Source Coding.
Digital Object Identifier 10.1109/TIT.2003.809480